Uterine remodelling during pregnancy and pseudopregnancy in the brushtail possum (*Trichosurus vulpecula*; Phalangeridae)

Melanie K. Laird,[1] (iD) Hanon McShea,[2] Bronwyn M. McAllan,[3] Christopher R. Murphy[4] and Michael B. Thompson[1]

[1]*School of Life and Environmental Sciences, University of Sydney, Sydney, NSW, Australia*
[2]*Department of Organismic and Evolutionary Biology, Harvard University, Cambridge, MA, USA*
[3]*Physiology, Faculty of Medicine, University of Sydney, Sydney, NSW, Australia*
[4]*Anatomy and Histology, Faculty of Medicine, University of Sydney, Sydney, NSW, Australia*

Abstract

The formation of a placenta is critical for successful mammalian pregnancy and requires remodelling of the uterine epithelium. In eutherian mammals, remodelling involves specific morphological changes that often correlate with the mode of embryonic attachment. Given the differences between marsupial and eutherian placentae, formation of a marsupial placenta may involve patterns of uterine remodelling that are different from those in eutherians. Here we present a detailed morphological study of the uterus of the brushtail possum (*Trichosurus vulpecula*; Phalangeridae) throughout pregnancy, using both scanning and transmission electron microscopy, to identify whether uterine changes in marsupials correlate with mode of embryonic attachment as they do in eutherian mammals. The uterine remodelling of *T. vulpecula* is similar to that of eutherian mammals with the same mode of embryonic attachment (non-invasive, epitheliochorial placentation). The morphological similarities include development of large apical projections, and a decrease in the diffusion distance for haemotrophes around the period of embryonic attachment. Importantly, remodelling of the uterus in *T. vulpecula* during pregnancy differs from that of a marsupial species with non-invasive attachment (*Macropus eugenii;* Macropodidae) but is similar to that of a marsupial with invasive attachment (*Monodelphis domestica;* Didelphidae). We conclude that modes of embryonic attachment may not be typified by a particular suite of uterine changes in marsupials, as is the case for eutherian mammals, and that uterine remodelling may instead reflect phylogenetic relationships between marsupial lineages.

Key words: epitheliochorial; marsupial; morphology; placenta; scanning electron microscopy; transmission electron microscopy; uterus.

Introduction

The mammalian placenta is a complex organ that supports embryonic growth and development within the uterus. Placentae vary considerably both between and within mammalian groups (Mossman, 1987; Murphy, 1998). The definitive placentae of eutherian mammals form from the allantois (chorioallantoic placenta; Wooding & Flint, 1994; Wildman, 2016). In contrast, marsupial placentae form from the yolk sac (choriovitelline placentae; Tyndale-Biscoe & Renfree, 1987; Freyer et al. 2002). Modes of embryonic attachment also vary considerably, even within mammalian families, and show a continuum of invasion of the uterus by the embryo (Wildman, 2016): from non-invasive epitheliochorial placentation (Ferner & Mess, 2011; Wildman, 2016) exhibited by eutherian ungulates (Ferner & Mess, 2011) and both macropodid and phalangerid marsupials (Tyndale-Biscoe & Renfree, 1987), to invasive endotheliochorial placentation and the highly invasive haemochorial placentation of rats and humans (Mess, 2014). Diversity in embryonic attachment is a likely driver of mammalian placental diversity (Wildman, 2016). In all cases studied thus far, formation of a placenta requires intimate contact between embryonic cells and a receptive uterine epithelium (Schlafke & Enders, 1975; Murphy, 2004; Wu et al. 2011). Receptivity can only occur under strict uterine conditions (Paria et al. 2002; Murphy, 2004) and involves remodelling of the uterine epithelium – termed the plasma membrane

transformation – to produce a brief window for attachment (Murphy, 2004; Zhang et al. 2013). This remodelling occurs irrespective of mode of embryonic attachment in eutherian mammals, but some specific cellular changes involved in receptivity often correlate with attachment mode. For example, many species with epitheliochorial placentation, including camels (Abd-Elnaeim et al. 1999), pigs (Dantzer, 1985) and roe deer (Aitken, 1975), develop large projections that increase the surface area for attachment. In contrast, species with haemochorial placentation, including rats and humans, undergo cell death and sloughing of regions of the uterine epithelium, which facilitate highly invasive implantation (Enders & Schlafke, 1967; Schlafke & Enders, 1975; Moffett & Loke, 2006). These differences suggest that specific modes of implantation necessitate particular uterine changes.

In contrast to eutherian mammals, uterine remodelling has been studied in detail in only a handful few marsupial species, including the dasyurid *Sminthopsis crassicaudata* (endotheliochorial placentation; Roberts & Breed, 1994; Laird et al. 2014), the didelphid *Monodelphis domestica* (endotheliochorial placentation; Zeller & Freyer, 2001) and the macropodid *Macropus eugenii* (epitheliochorial placentation; Freyer et al. 2003). Marsupial pregnancy differs from that of eutherian mammals in several important respects (Zeller & Freyer, 2001; Freyer & Renfree, 2009). In addition to placental differences, gestation is relatively short and is shorter than the oestrous cycle (Carter, 2008; McAllan, 2011). Young are born extremely altricial and most organ growth and development occurs after birth during an extended lactation period in the pouch (McAllan, 2003; Shaw & Renfree, 2006). In addition, marsupial embryos are surrounded by a shell coat (Renfree & Shaw, 2000; Ferner & Mess, 2011) until they implant late in their gestation (approximately two-thirds of the way through; Rothchild, 2003) relative to eutherian embryos. The relationship between uterine remodelling and mode of embryonic attachment in marsupial pregnancy is unknown, but given the major differences between marsupial and eutherian pregnancy, we predict that uterine remodelling is not influenced by mode of embryonic attachment in marsupials, unlike in eutherian mammals.

We describe morphological changes to the uterine epithelium of the brushtail possum (*Trichosurus vulpecula*) throughout pregnancy using both scanning and transmission electron microscopy. Like *M. eugenii*, *T. vulpecula* has epitheliochorial (non-invasive) placentation (Pilton & Sharman, 1962). Thus *T. vulpecula* is ideal for comparison with other marsupial species so far studied to identify possible relationships between uterine morphology and mode of placentation. We predict that the uterus of *T. vulpecula* undergoes remodelling in preparation for pregnancy, but that the specific cellular changes are different from those of other mammalian species with epitheliochorial placentation.

Materials and methods

Study species

Trichosurus vulpecula has an oestrous cycle of 28 days (Tyndale-Biscoe, 2005) and a 17.5-day gestation period (Pilton & Sharman, 1962). Ovulation alternates between ovaries and only one uterus carries an embryo at a time (monovular; Renfree, 2000; Sizemore et al. 2004; Tyndale-Biscoe, 2005). As is the case for most marsupials, and unlike in eutherians, conception does not affect the course of the oestrous cycle in *T. vulpecula* (Tyndale-Biscoe & Renfree, 1987). Ovarian, hormonal and gross uterine changes are similar during both pregnancy and the non-pregnant oestrous cycle in *T. vulpecula* (Pilton & Sharman, 1962). Hence, a pseudopregnancy (luteal phase occurring in the non-pregnant uterus; Pilton & Sharman, 1962), which is largely indistinguishable from a pregnancy, occurs as a part of every normal oestrous cycle. Ovulation of a single egg occurs 1–2 days after oestrus and attachment of the embryo occurs approximately 14 days after conception, with birth 3–4 days later (Tyndale-Biscoe, 2005). In females that give birth, lactation suppresses ovulation until the young leaves the pouch at approximately 110 days post-oestrus, at which time the female can again enter oestrus.

Tissue collection and processing

Uterine and ovarian tissues of female brushtail possums were collected opportunistically from a cull undertaken with animal ethics permission from Landcare Research, New Zealand (AEC approval no. 12/02/01) in the Orongorongo Valley near Wellington, New Zealand. The main breeding season for brushtail possums in New Zealand occurs from February to April (Tyndale-Biscoe, 1955; Crawley, 1973). Tissues were collected over two seasons (April 2014 and March 2015) to obtain a complete set of reproductive stages. Tissues were collected from a total of 18 females (17 cycling, one juvenile). Ovaries were fixed in 10% neutral buffered formalin for 24 h and stored in 70% ethanol (EtOH). Uterine tissue was excised and processed for scanning electron microscopy (SEM) and transmission electron microscopy (TEM).

Light microscopy of ovaries and reproductive staging

Whole ovaries were gradually dehydrated to 100% EtOH and then embedded in paraffin. Paraffin blocks were serially sectioned at 7 μm using a Tissue-Tek Accu-Cut™ microtome (Sakura, Tokyo, Japan) and sections were mounted on gelatin-coated slides and stained with haematoxylin and eosin (Drury & Wallington, 1980). Images were captured using an Olympus DX-53 digital microscope (Olympus, Tokyo, Japan). Sections were examined for the presence of follicles and corpora lutea (ovulated follicles; Shorey & Hughes, 1973; Selwood & Woolley, 1991) and the maximal size of each corpus luteum was measured using CellSens software. The stage of the oestrous cycle of each female (approximate number of days post-oestrus) was estimated using maximal corpus luteal sizes and gross reproductive tract morphology, including relative size and vascularization of uteri and the vaginal cul-de-sac (e.g. Crawford et al. 1997, 1999), and the relative size difference between the gravid and non-gravid uterus (e.g. Pilton & Sharman, 1962). Females with similar ovarian and uterine morphology were grouped together into one of five stages post-oestrus: Stage 1 (0–6 days post-oestrus; $n = 5$), Stage 2 (7–11 days post-oestrus; $n = 5$), Stage 3 (11–13 days

post-oestrus; *n* = 3), Stage 4 (13–17.5 days post-oestrus; *n* = 3), Stage 5 (> 17.5 days post-oestrus; *n* = 1). Four females from Stages 2 and 3 were confirmed pregnant, as embryos were found in the uterus. The ovarian and uterine changes of pseudopregnant females are indistinguishable from those of pregnancy until after 12 days post-oestrus, when relative differences in size and vasculature of pregnant and pseudopregnant uteri appear (Pilton & Sharman, 1962). Hence, pregnant and pseudopregnant females at the same stage post-oestrus were grouped together where applicable. One juvenile female (anoestrus) is included for comparison with cycling females.

Transmission electron microscopy (TEM)

Uterine tissue for TEM was fixed in 2.5% glutaraldehyde in 0.1 M phosphate buffer (PB) for 2 h then rinsed in 0.1 M PB. Samples were post-fixed for 1 h in 4% osmium tetroxide (OsO_4) with 0.8% potassium ferrocyanide [$K_4Fe(CN)_6$] to enhance membrane contrast (Hulstaert et al. 1983), followed by thorough rinsing in 0.1 M PB, then 50% EtOH and 70% EtOH, and further dehydration to 100% EtOH. Samples were cut into pieces of approximately 0.5 mm^3 and slowly infiltrated with Spurr's resin (Agar Scientific, Essex, UK) in increments of 25%. Tissue pieces were then polymerized at 62 °C overnight in individual BEEM® capsules. A Leica Ultrastat 7 cryostat (Leica, Heerbrugg, Switzerland) was used to cut semithin (200 μm) and ultrathin (70 μm) sections, and ultrathin sections were transferred to 200-μm mesh copper grids (ProSci Tech, Queensland, Australia). Sections on grids were post-stained by flotation of each grid on a drop of 2% uranyl acetate for 10 min, thorough rinsing in warm water, then floating on a drop of Reynolds lead citrate surrounded by sodium hydroxide (NaOH) pellets for 10 min, followed by further rinsing (Hayat, 1986). Grids were allowed to air dry before imaging using a Zeiss Sigma HD VP STEM (Zeiss, Oberkochen, Germany). Images were collected from at least two grids from each of three blocks of tissue per female.

Scanning electron microscopy (SEM)

Uterine tissue for SEM was dissected to expose the interior surface. Samples were fixed in 2.5% glutaraldehyde in 0.1 M PB for 2 h, thoroughly rinsed in 0.1 M PB, then post-fixed in 4% osmium tetroxide (OsO_4) for 1 h (4 drops osmium and 15 drops 0.1 M PB), followed by rinsing in 0.1 M PB, distilled water, 50% EtOH, and 70% EtOH. Samples were gradually dehydrated to 100% EtOH as for TEM tissue, and dried using a Leica EM CPD300 Critical Point Dryer (Leica, Wetzlar, Germany) using carbon dioxide as the drying agent. Samples were then mounted onto aluminium stubs with a layer of carbon tape and coated with a 15-nm layer of gold. Images were captured on a JEOL NeoScope JCM-600 Tabletop SEM (Tokyo, Japan) and a Zeiss Sigma HD VP STEM (Zeiss, Oberkochen, Germany).

Cellular composition

The cellular composition of the uterine surface was identified by comparing the relative abundance of distinct cell types throughout pregnancy. Scanning electron micrographs were taken of at least three uterine regions per animal, between 500× and 2000×. Each cell in an image was allocated to a cell type, although damaged cells, or cells that could not be clearly identified, were not counted. Proportions were obtained by dividing the total number of each cell type by the total number of cells in the image. Proportions for each animal were arcsine-transformed (Dytham, 2011). The analysis was applied until SEM < 0.05 for each cell type for each animal (Aherne & Dunhill, 1982).

Results

Light microscopy of ovaries

Ovaries of all cycling females contained a corpus luteum and numerous primordial, primary and secondary follicles (Fig. 1). Immediately following oestrus (Stage 1; Fig. 1A), the average maximum corpus luteum diameter was 160 ± 22 μm, increasing to 1730 ± 233 μm by the start of the luteal phase (Stage 2; Pilton & Sharman, 1962; Fig. 1B) and 3593 ± 314 μm by Stage 3 (Fig. 1C). The greatest average diameter of the corpus luteum occurred during Stage 4 (4469 ± 137 μm), whereas the diameter of the post-partum corpus luteum was 3425 μm.

Electron microscopy of uteri

Stage 1: 0–6 days post-oestrus
The uterine surface is flattened, with many visible gland openings (Fig. 2A). Uterine epithelial cells at this stage are uniform and form a single layer of columnar cells with large nuclei located in the mid-cytoplasm (Fig. 2A,B). Cell apices are flattened or slightly domed with occasional sparse microvilli (Fig. 2C,D). Most cells have prominent raised cell borders, and no ciliated cells are present. The basal plasma membranes of uterine epithelial cells are highly folded. Cells at this stage also possess relatively few organelles, although rounded mitochondria are prominent in secretory cells (Fig. 2D) and some cells possess small secretory droplets. Densely packed stromal cells immediately underlie the uterine epithelium and large blood vessels occur deep in stromal tissue (Fig. 2E). Glandular epithelial cells, such as luminal epithelial cells, form a single layer of uniform columnar cells, although the basal plasma membranes of these cells are not folded.

Stage 2: 7–11 days post-oestrus
The uterine surface is folded at this stage (Fig. 3A) and uterine epithelial cells are more irregular than at Stage 1 (Fig. 3B). Cells in some areas are pseudostratified columnar (Fig. 3B). Cell apices are more rounded than at Stage 1 (Fig. 3C) and possess sparse microvilli covered in glycocalyx fibres (Fig. 3B). Scattered ciliated cells are dispersed among the microvillous cells (Fig. 3C). Luminal cells are domed and secretory in appearance near the openings of uterine glands. Some secretory droplets occur in the uterine lumen (Fig. 3B). The stromal area around these vesicles is largely devoid of cells, with fewer stromal cells overall than previously (Fig. 3D). Glandular epithelial cells are elongated and pseudostratified columnar by this stage and are secretory
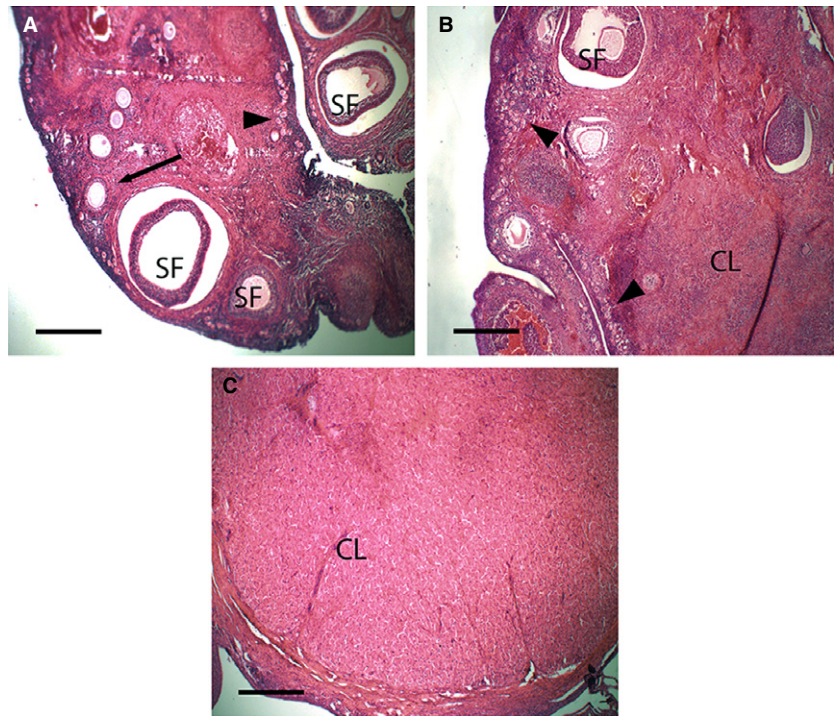
Fig. 1 Light micrographs of histological sections of ovaries of *Trichosurus vulpecula*. (A) Stage 1 (0–6 days post-oestrus), (B) Stage 2 (7–11 days post-oestrus), (C) Stage 3 (11–13 days post-oestrus). Primordial follicles (arrowheads), primary follicles (arrow) and secondary follicles (SF) occur at all stages post-oestrus. The corpus luteum (CL) becomes prominent in Stages 2 and 3 post-oestrus. Sections stained with haematoxylin and eosin; Scale bar: 400 μm.

(Fig. 3E). Blood vessels underlie the uterine epithelium (Fig. 3D).

Stage 3: 11–13 days post-oestrus

By Stage 3, most uterine epithelial cells are rounded with domed apices (Fig. 4A,B), and many have short spiky microvilli (Fig. 4A). These cells are secretory in appearance and some even appear to be budding off into the uterine lumen (Fig. 4C,D). These cells are pseudostratified columnar and elongated relative to previous stages (Fig. 4D). Abundant organelles and secretory vesicles are present in the cytoplasm, particularly rounded mitochondria, dark-staining vesicles in the apical region, and elongated nuclei (Fig. 4B). Glands are not obvious in the stroma at this stage.

Stage 4: 13–17.5 days post-oestrus

By this stage, the uterine surface is more folded than for previous stages. Uterine epithelial cells form a mixed population of cells with short microvilli, ciliated cells, and domed protruding cells (Fig. 5A,B). These domed cells appear highly secretory, as for the previous stage, but protrude further into the uterine lumen (Fig. 5B,C). Uterine epithelial cells possess large pale nuclei and numerous round mitochondria (Fig. 5C). Some cells also have large lipid-filled vesicles, and scattered smaller vesicles (Fig. 5C). Scattered pale degenerative cells occur in the uterine epithelium by this stage. Blood vessels underlie the uterine epithelium (Fig. 5D), although some are distorted. In some regions of the uterus, endothelial and stromal cells are interspersed

(Fig. 5C), particularly where luminal cells are extremely domed. As for Stage 2, large vacuoles occur in the stroma, which by this stage almost displace the uterine epithelium, as well as some long, thin stromal cells and abundant acellular material (Fig. 5C). No obvious glands occur in the stroma at this stage.

Stage 5: > 17.5 days post-oestrus (postpartum)

The uterine surface is flattened relative to previous stages and cells are less domed than previously (Fig. 6A), forming a mixed population of cells similar to Stage 4. Some larger cells possess short spiky microvilli (Fig. 6A,B). Numerous ciliated cells are scattered throughout (Fig. 6B) and these contain abundant small round mitochondria and prominent basal bodies (Fig. 6C). Many small secretory droplets occur in the uterus (Fig. 6B). Some regions of the uterus are highly secretory (Fig. 6D). Cells in these regions are highly disorganized and appear to be actively shedding cytoplasmic material into the lumen. Occasional intercellular spaces occur (Fig. 6D).

Anoestrus – juvenile female

The uterine surface is folded with numerous gland openings and ciliated cells (Fig. 7A). Uterine epithelial cells are pseudostratified columnar and extremely elongated and irregular (Fig. 7B). The cytoplasm of these cells is denser than for cycling females, with an elongated nucleus, numerous secretory vesicles and round mitochondria in the apical region of the cytoplasm (Fig. 7B). The uterine stroma is tightly packed with cells.
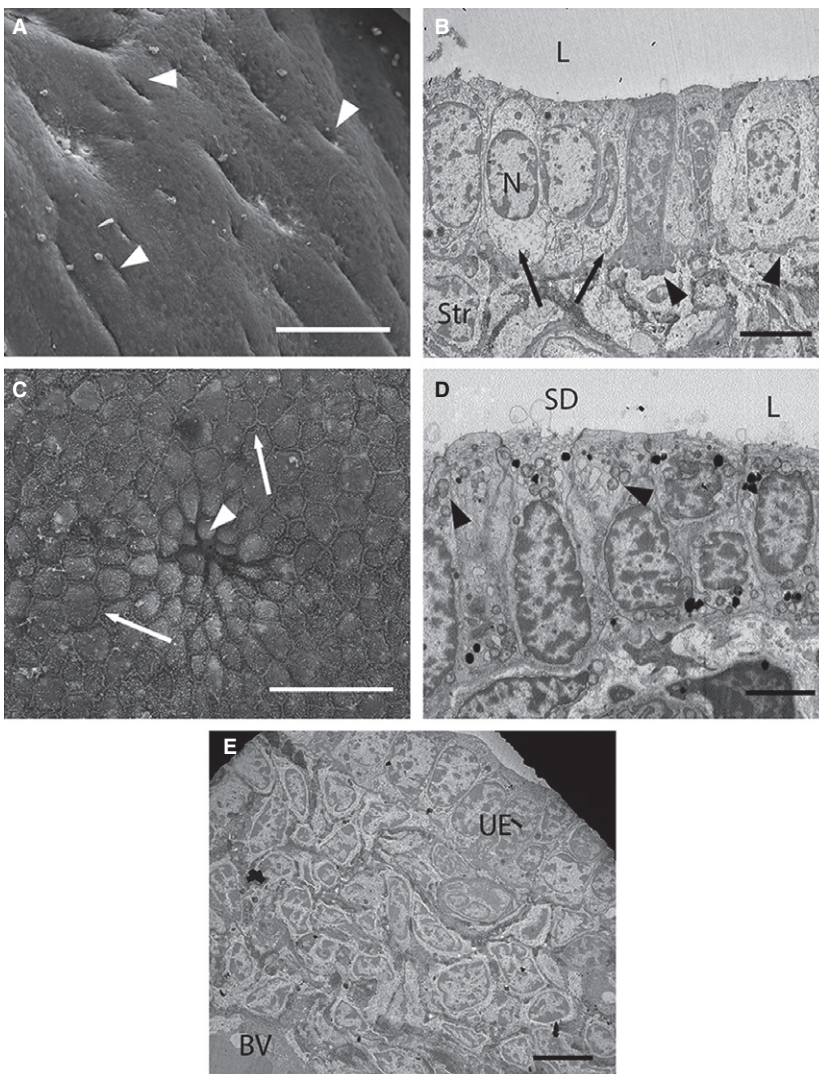
Fig. 2 Electron micrographs of uterine cells at Stage 1 (approximately 1–6 days post-oestrus) in *Trichosurus vulpecula*. (A,C) Scanning electron micrographs. (B,D,E) Transmission electron micrographs. (A) The uterine surface is smooth with numerous gland openings (arrowheads). Scale bar: 100 μm (SEM). (B) Uterine epithelial cells (arrows) are uniform and form a single layer of columnar cells with round central nuclei (N). Stromal cells (Str) are densely packed below the uterine epithelium. The basal plasma membrane is also highly folded (arrowheads). L, lumen. Scale bar: 5 μm (TEM). (C) Cells have slightly domed apices, particularly near a gland opening (arrowhead) and prominent cell borders (arrows). Scale bar: 20 μm (SEM). (D) Some luminal cells are secretory (secretory droplets, SD), and contain numerous rounded mitochondria (arrowheads). L, lumen. Scale bar: 4 μm (TEM). (E) Large blood vessels (BV) occur deep in stromal tissue at this stage. UE, uterine epithelium. Scale bar: 5 μm (TEM).

Cellular composition

Five cell types were identified on the uterine surface: bare surface, sparse microvilli, dense microvilli, blebbing cells and ciliated cells (Fig. 8A). Immediately post-oestrus (Stage 1), bare and sparsely microvillous cells dominate the uterine surface (Fig. 8B). The uterine epithelium becomes progressively more heterogeneous, leading up to implantation as ciliated and blebbing cells become common. Postpartum, the population of cells resembles that of Stage 2.

Discussion

Uterine remodelling occurs throughout pregnancy and pseudopregnancy in *T. vulpecula* (Fig. 9). Ovulation and formation of a corpus luteum occur 1–2 days after oestrus in *T. vulpecula* (Tyndale-Biscoe, 2005) and uterine epithelial cells in this post-oestrus proliferative phase are distinctly flattened and uniform. These cells become less uniform with domed apices by the start of the luteal phase approximately 7 days post-oestrus (Stage 2), corresponding to formation of the unilaminar blastocyst (Pilton & Sharman, 1962) and maximal size and vascularization of the uterus (Crawford et al. 1997). By 13 days post-oestrus (Stage 3), luminal epithelial cells are even more domed, elongated and actively secreting, coinciding with a period of rapid blastocyst expansion (Pilton & Sharman, 1962; Hughes & Hall, 1984). Dramatic cellular changes occur around the time of shell coat rupture and attachment of the embryo to the uterine wall (approximately 14.5 days post-oestrus; Stage 4; Hughes & Hall, 1984), when blood vessels come to underlie the uterine epithelium, and the apices of luminal epithelial cells are extremely domed and project into the lumen. Cells maintain this secretory morphology for the remainder of pregnancy.

Uterine remodelling is most extensive, leading up to rupture of the shell coat in *T. vulpecula* (Stage 3). Substantial remodelling during this period also occurs in the didelphid
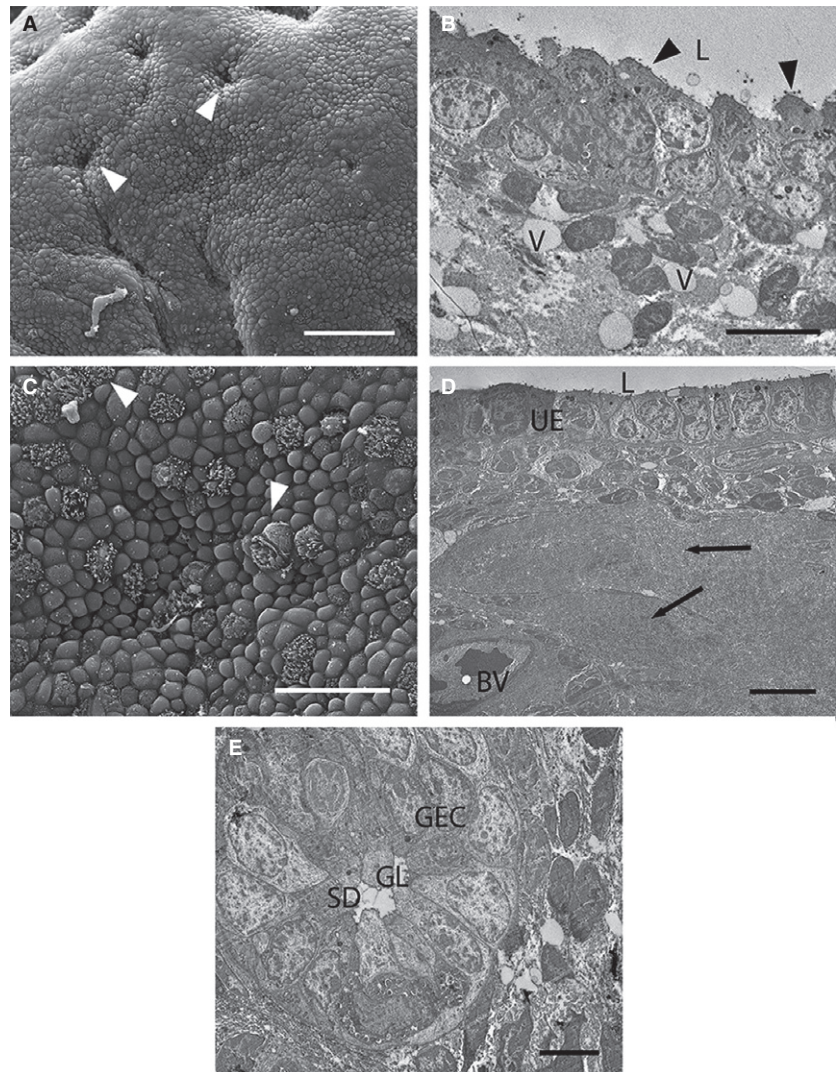
Fig. 3 Electron micrographs of uterine cells at Stage 2 (approximately 7–11 days post-oestrus) in *Trichosurus vulpecula*. (A,C) Scanning electron micrographs. (B,D,E) Transmission electron micrographs. (A) The uterine surface is folded by this stage, but still with numerous gland openings (arrowheads). Scale bar: 50 μm (SEM). (B) Uterine epithelial cells are less uniform than previously, with round apices and short blunt microvilli (arrowheads). Fluid-filled vesicles (V) occur among the stromal cells. L, lumen. Scale bar: 5 μm (TEM). (C) Cell apices are domed relative to previously and ciliated cells (arrowheads) are scattered among microvillous cells. Scale bar: 20 μm (SEM). (D) Blood vessels (BV) occur closer to the uterine epithelium (UE). Parts of the stroma are filled with an acellular fluid material (arrows). L, lumen. Scale bar: 10 μm (TEM). (E) Glandular epithelial cells (GEC) are pseudostratified and project into the glandular lumen (GL). SD, secreted droplets. Scale bar: 5 μm (TEM).

Monodelphis domestica (endotheliochorial placentation) which, like *T. vulpecula*, develops highly domed and secretory luminal epithelial cells (Zeller & Freyer, 2001). Luminal cells of the macropodid, *M. eugenii* (epitheliochorial placentation)*,* also become domed and rounded, although not secretory (Freyer et al. 2002), and those of the dasyurid, *S. crassicaudata* (endotheliochorial placentation), develop complex apical structures thought to increase the surface area for attachment (Laird et al. 2014). The marsupial shell coat acts as a physical barrier between the embryo and the uterine environment for most of pregnancy (Renfree & Shaw, 2000). Hence, remodelling leading up to shell coat rupture is expected in the marsupial uterus, as the majority of nutrient uptake occurs after hatching, when the embryo can directly interact with maternal cells (Renfree & Shaw, 2000). Uterine epithelial remodelling is also similar to that of the vaginal cul-de-sac epithelium before ovulation in *T. vulpecula* (Crawford et al. 1999). Remodelled cul-de-sac

cells are dramatically elongated with a 17-fold greater cytoplasmic volume than at the start of the oestrous cycle (Crawford et al. 1999). Dramatic cellular changes throughout the reproductive tract demonstrate that epithelial remodelling is critical to reproductive success in *T. vulpecula*.

Cellular diversity of the uterine epithelium increases leading up to implantation in *T. vulpecula*. Immediately post-oestrus, the uterine epithelium consists predominantly of bare or sparsely microvillous cells, whereas densely microvillous, ciliated, and blebbing cells become increasingly common in later stages. The epithelium then begins to revert to the non-receptive state postpartum. These findings are consistent with the previous finding that both progesterone and oestradiol promote ciliogenesis and an increase in microvillar density in the uterus of *T. vulpecula* (Shorey & Hughes, 1973; Arnold & Shorey, 1985; Sizemore et al. 2004). Increasing heterogeneity in the uterine epithelium
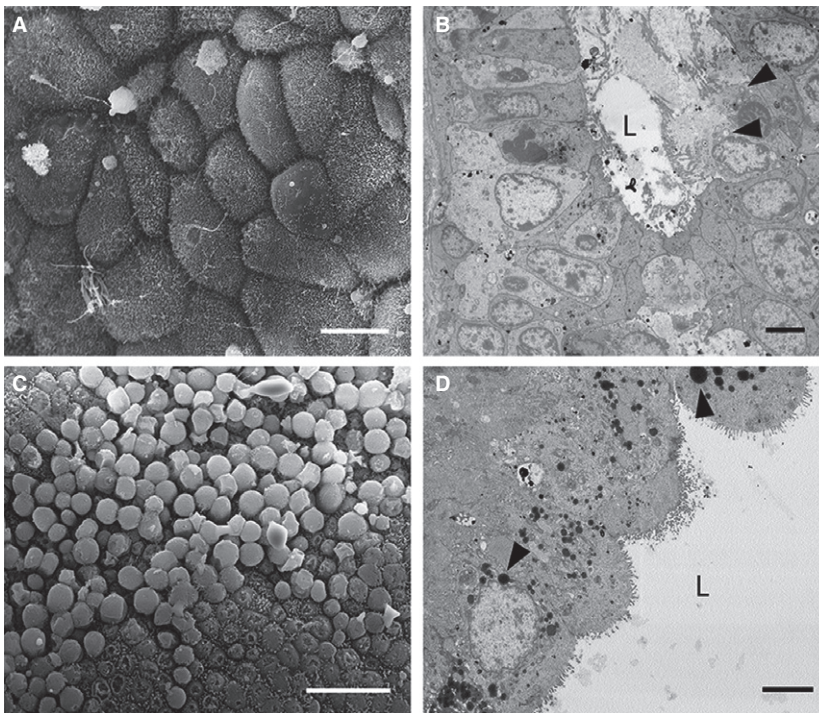
Fig. 4 Electron micrographs of uterine cells at Stage 3 (approximately 11–13 days post-oestrus) in *Trichosurus vulpecula*. (A,C) Scanning electron micrographs. (B,D) Transmission electron micrographs. (A) Uterine epithelial cells remain domed and possess short spiky microvilli. Scale bar: 10 μm (SEM). (B) Some cells are secretory and release their cytoplasmic contents into the uterine lumen (L). These cells have extremely enlarged rounded mitochondria (arrowheads). Scale bar: 4 μm (TEM). (C) SEM surface view of a similar region to (B) showing extremely domed epithelial cells; Scale bar: 20 μm. (D) Uterine cells contain abundant organelles by this stage, including round mitochondria (arrowheads) and small lipid droplets. L, lumen. Scale bar: 4 μm (TEM).

throughout pregnancy is unexpected, as remodelling in rodents (Murphy et al. 2000), ungulates (Wooding & Morgan, 1995; Murphy et al. 2000), rabbits (Winterhager & Denker, 1990), bats (Potts & Racey, 1971), and the marsupial species *S. crassicaudata*, results in a uniform, flattened and well-ordered epithelial layer (Murphy et al. 2000; Laird et al. 2014). In these species, uniformity is thought to facilitate close apposition to, and in some cases invasion of, the uterine epithelium by the embryo (Murphy et al. 2000; Laird et al. 2014). Since embryos of *T. vulpecula* only superficially interact with the uterine epithelium (Hughes, 1974), a heterogeneous uterine epithelium, with cells presumably capable of diverse functions (Shorey & Hughes, 1973), may be required to maintain embryos which do not implant invasively.

Gland abundance and secretory activity declines in late pregnancy in *T. vulpecula,* as both glands and stromal cells become progressively less common from 11 to 13 days post-oestrus. Gland abundance also decreases during pregnancy in many mammal species (Abd-Elnaeim et al. 1999; Zeller & Freyer, 2001; Freyer et al. 2002; Freyer & Renfree, 2009), and typically reflects a shift from histotrophic nutrient provision to the embryo (i.e. material secreted by uterine glands; Wildman, 2016) to haemotrophic nutrient provision (i.e. secretion of material from the maternal blood circulation by luminal epithelial cells; Wildman, 2016). Initial pre-attachment development of mammalian embryos is supported by histotrophes from uterine glands (Wooding & Burton, 2008), whereas haemotrophes support growth post-attachment, either through direct embryonic contact

with maternal blood, or diffusion/active transport of haemotrophes from maternal blood followed by secretion by the uterine epithelium into the uterine lumen (Freyer et al. 2003). As implantation in *T. vulpecula* is not invasive, the dramatic increase in luminal epithelial cell secretion, which precedes shell coat rupture, suggests that a shift from histotrophic to haemotrophic nutrient provision also occurs in this species (Zeller & Freyer, 2001). This hypothesis is supported by uterine modifications in *T. vulpecula* during pregnancy that also facilitate transfer of haemotrophes in other mammalian species with epitheliochorial placentation (Abd-Elnaeim et al. 1999), including migration of blood vessels closer to the uterine epithelium (Stage 4), development of deep folds in the basal plasma membrane of uterine epithelial cells, and an increase in abundance of ciliated and densely microvillous cells in the uterine epithelium at Stages 3 and 4, which increase the cell surface area for secretion (Sizemore et al. 2004). After shell coat rupture, blood vessels in some regions break down and release fluid and blood cells into the stroma, which may then be transported directly into the uterine lumen transcellularly via bulk flow (Fig. 5C).

The changes involved in uterine remodelling in *T. vulpecula*, including development of large uterine projections and modifications to support haemotrophic transfer, are thus generally consistent with those of eutherian mammals with epitheliochorial (non-invasive) placentation, including camels (Abd-Elnaeim et al. 1999), sheep (Guillomot et al. 1981) and pigs (Dantzer, 1985). This finding suggests a relationship between morphology and placental mode in
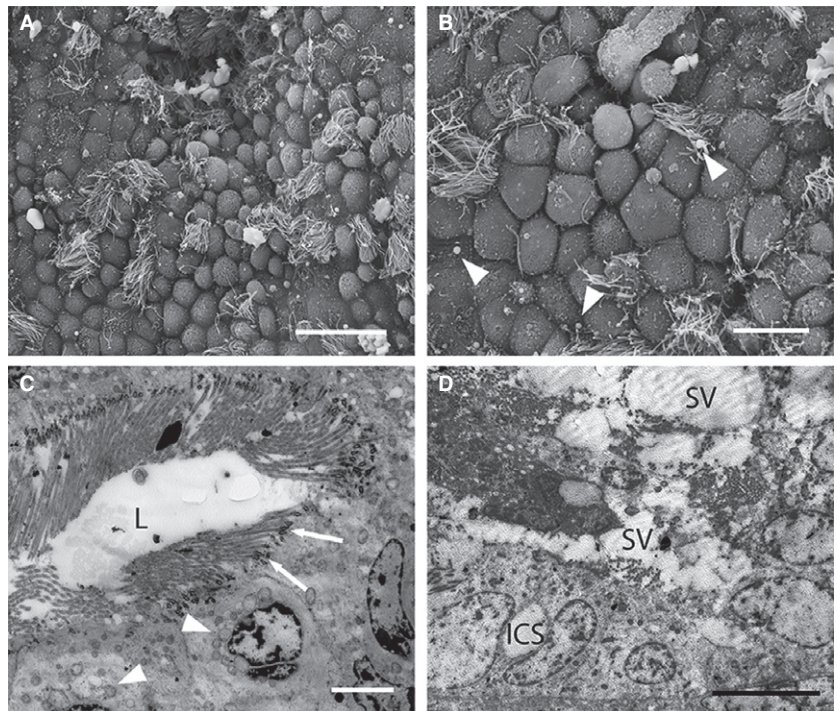
Fig. 5 Electron micrographs of uterine cells at Stage 4 (approximately 13–17.5 days post-oestrus) in *Trichosurus vulpecula*. (A,B) Scanning electron micrographs. (C,D) Transmission electron micrographs. (A) Extremely domed epithelial cells are more common in the uterus by this stage. Scale bar: 100 μm (SEM). (B) Uterine cells are highly secretory in appearance and project far into the uterine lumen. Scale bar: 20 μm (SEM). (C) Cross-section through a similar region to B). Cells are extremely domed and elongated and contain very large lipid droplets (LD). Large regions of fluid underlie the uterine epithelium, and blood cells (arrows) come into close contact with epithelial cells. L, lumen. Scale bar: 10 μm (TEM). (D) Large blood vessels (BV) lie close to, and distort, the uterine epithelium. L, lumen. Scale bar: 4 μm (TEM).
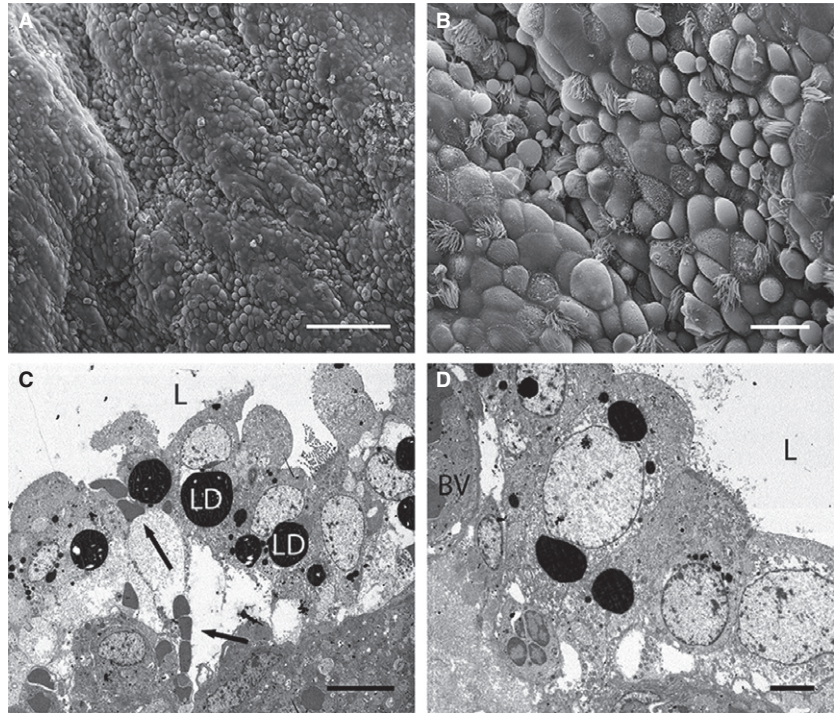
marsupials, which is unexpected, given the different reproductive strategies used by eutherian mammals and marsupials. However, this hypothesis is not supported by the morphological changes of other marsupial species. For example, similarities occur between uterine changes in *T. vulpecula* and *M. eugenii* (epitheliochorial placentation),

including migration of blood vessels towards the luminal surface and folding of the basal plasma membrane of luminal cells; however, remodelling in these two species differs in several important ways. In contrast to *T. vulpecula*, pregnancy in *M. eugenii* involves an extended phase of glandular secretion, which continues until birth (Renfree, 1980;

Fig. 6 Electron micrographs of uterine cells at Stage 5 (approximately > 17.5 days post-oestrus, postpartum) in *Trichosurus vulpecula*. (A,B) Scanning electron micrographs. (C,D) Transmission electron micrographs. (A) Uterine epithelial cells are still domed postpartum but much less so than previous stages. The uterine surface is relatively flattened. Scale bar: 20 μm (SEM). (B) Small secreted droplets (arrowheads) occur in the uterus. Both ciliated and microvillous cells are present. Scale bar: 10 μm (SEM). (C) Numerous ciliated cells occur in the uterus postpartum. These contain small round mitochondria (arrowheads) and extremely prominent basal bodies associated with the cilia (arrows). Scale bar: 4 μm (TEM). (D) Large secretory vesicles (SV) occur in the uterine lumen, along with cellular debris. Intercellular spaces (ICS) were occasionally seen between adjacent uterine epithelial cells. Scale bar: 10 μm (TEM).
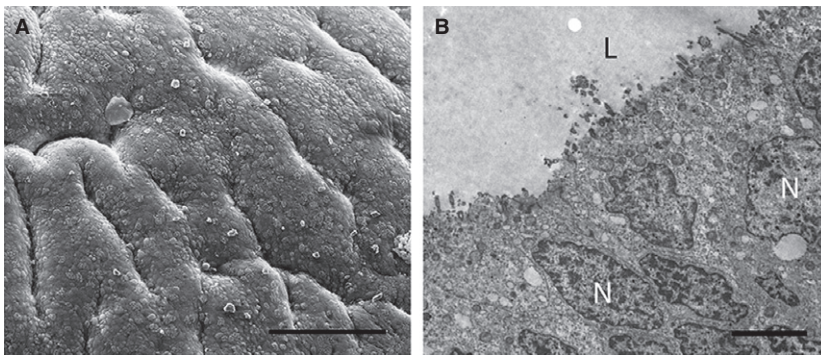
Fig. 7 Electron micrographs of epithelial cells in the uterus of *Trichosurus vulpecula* (juvenile female). (A) The uterine surface is folded, with deep ridges; Scale bar: 100 μm (SEM). (B) Uterine cells are pseudostratified with irregularly shaped nuclei (N) and solitary cilia (TEM). L, lumen. Scale bar: 3 μm.
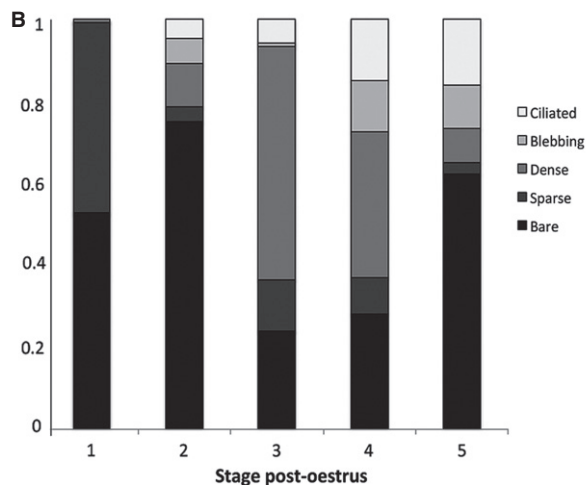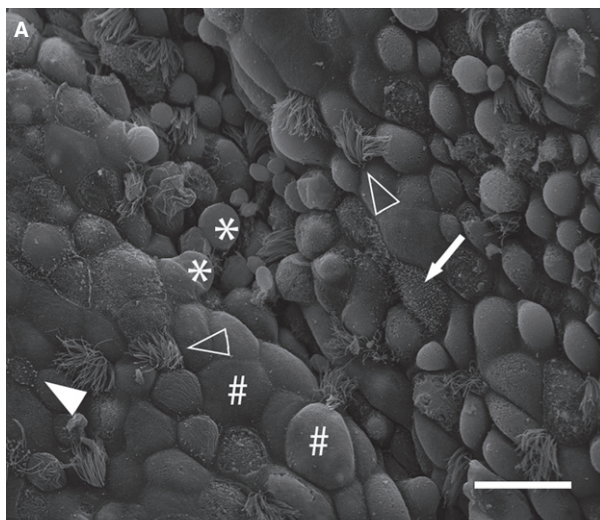

Fig. 8 Cellular composition of the uterine epithelium of *Trichosurus vulpecula*. (A) Scanning electron micrograph depicting representatives of the five distinct cell types: bare cells (#), sparse microvilli (filled arrowhead), dense microvilli (arrow), blebbing cells (*), ciliated cells (open arrowheads); Scale bar: 20 μm. (B) Relative proportions of each cell type on the uterine surface throughout pregnancy. Data are presented as means of arcsine-transformed proportions for each stage of pregnancy (SEM < 0.05).
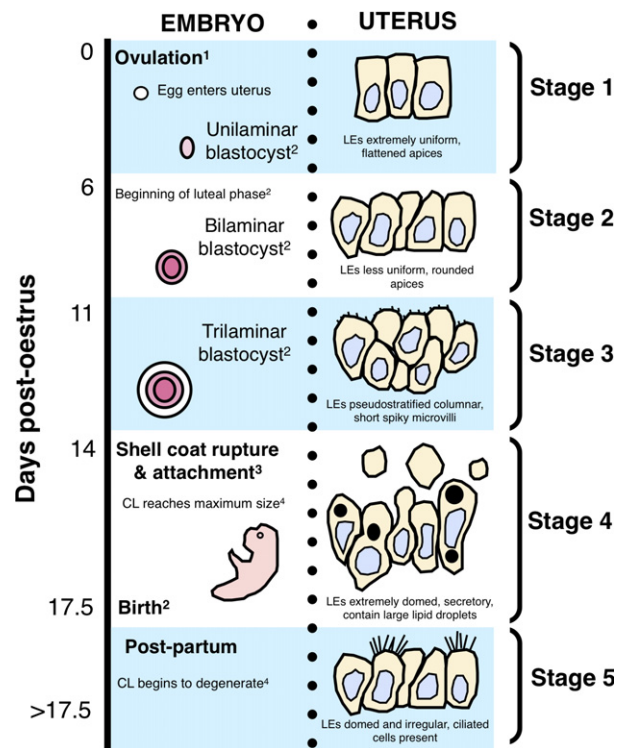

Fig. 9 Summary of changes to uterine epithelial cell morphology of *Trichosurus vulpecula* aligned with major ovarian and embryonic events during pregnancy; LEs, luminal epithelial cells; CL, corpus luteum. [1]Tyndale-Biscoe (2005); [2]Pilton & Sharman (1962); [3]Hughes & Hall (1984); [4]Shorey & Hughes (1973).

Freyer et al. 2002), while minimal luminal cell secretion occurs. Hence, unlike *T. vulpecula*, both histotrophic and haemotrophic nutrition support embryonic development after attachment in *M. eugenii* (Freyer et al. 2002). In addition, *M. eugenii* displays maternal recognition of pregnancy, as the endometrium proliferates only in response to the presence of an embryo (Renfree, 2000; Freyer et al. 2002), whereas in *T. vulpecula*, uterine remodelling occurs in both the pregnant and non-pregnant oestrous cycle. Interestingly, uterine changes in *T. vulpecula* are similar to

those of *M. domestica*, which has invasive endotheliochorial placentation, as *M. domestica* also demonstrates many of the uterine changes typical of eutherian species with non-invasive implantation (Freyer & Renfree, 2009). Thus although uterine morphology during pregnancy in *T. vulpecula* is consistent with that of eutherian mammals with the same placental mode, variability in uterine morphology among marsupial species suggests that morphology may not be related to placental type in marsupials.

Marsupials in the clade Didelphidae (including *M. domestica*) are ancestral and display reproductive traits of the marsupial common ancestor (Freyer et al. 2003). Many of these traits also characterize pregnancy in the clade Phalangeridae (including *T. vulpecula*), particularly a decrease in histotrophic nutrition and a lack of maternal recognition of pregnancy (Freyer et al. 2003). In contrast, macropodids (including *M. eugenii*), display many derived reproductive characteristics (Freyer et al. 2003). As the marsupial common ancestor likely had invasive implantation (Zeller & Freyer, 2001; Freyer et al. 2003), non-invasive attachment has most likely arisen independently in phalangerids and macropodids. Hence, differences in uterine remodelling among marsupial species with non-invasive attachment may reflect different evolutionary histories. Comparison of uterine changes between marsupial species demonstrates that much of the uterine remodelling in marsupials, unlike eutherian mammals, may not be related to mode of attachment and may instead reflect evolutionary relationships between marsupial lineages.

Acknowledgements

Author contributions

M.K.L. carried out the sample preparation and electron microscopy and wrote the manuscript. H.M. carried out the sample preparation and light microscopy of ovaries and contributed to the manuscript. M.B.T., C.R.M. and B.M.M. contributed to experimental design, technical advice, image interpretation and manuscript preparation and revision.

Conflict of interest

The authors have no conflicts of interest to declare.

References

Abd-Elnaeim MM, Pfarrer C, Saber AS, et al. (1999) Fetomaternal attachment and anchorage in the early diffuse epitheliochorial placenta of the camel (*Camelus dromedarius*). *Cells Tissues Organs* **164**, 141–154.

Aherne WA, Dunhill MS (1982) *Morphometry*. London: Arnold.

Aitken RJ (1975) Ultrastructure of the blastocyst and endometrium of the roe deer (*Capreolus capreolus*) during delayed implantation. *J Anat* **119**, 369–384.

Arnold R, Shorey CD (1985) Structure of the uterine luminal epithelium of the brush-tailed possum (*Trichosurus vulpecula*). *J Reprod Fertil* **74**, 565–573.

Carter AM (2008) What fossils can tell us about the evolution of viviparity and placentation. *Placenta* **29**, 930–931.

Crawford JL, Shackell GH, Thompson EG, et al. (1997) Preovulatory follicle development and ovulation in the brushtail possum (*Trichosurus vulpecula*) monitored by repeated laparoscopy. *J Reprod Fertil* **110**, 361–370.

Crawford JL, McLeod BJ, Hurst PR (1999) Cyclical changes in epithelial cells of the vaginal cul-de-sac of brushtail possums (*Trichosurus vulpecula*). *Anat Rec* **254**, 307–321.

Crawley M (1973) A live-trapping of Australian brush-tailed possums, *Trichosurus vulpecula* (Kerr), in the Orongorongo Valley, Wellington, New Zealand. *Aust J Zool* **21**, 75–90.

Dantzer V (1985) Electron microscopy of the initial stages of placentation in the pig. *Anat Embryol* **172**, 281–293.

Drury RAB, Wallington EA (1980) *Carleton's Histological Technique*, 5th edn. Oxford: Oxford University Press.

Dytham C (2011) *Choosing and Using Statistics: A Biologist's Guide*, 3rd edn. Chichester: Wiley-Blackwell Publishing.

Enders AC, Schlafke S (1967) A morphological analysis of the early implantation stages in the rat. *Am J Anat* **120**, 185–226.

Ferner K, Mess A (2011) Evolution and development of fetal membranes and placentation in amniote vertebrates. *Respir Physiol Neurobiol* **178**, 39–50.

Freyer C, Renfree MB (2009) The mammalian yolk sac placenta. *J Exp Zool* **312**, 545–554.

Freyer C, Zeller U, Renfree MB (2002) Ultrastructure of the placenta of the tammar wallaby, *Macropus eugenii*: comparison with the gray short-tailed opossum, *Monodelphis domestica*. *J Anat* **201**, 101–119.

Freyer C, Zeller U, Renfree MB (2003) The marsupial placenta: a phylogenetic analysis. *J Exp Zool* **299A**, 59–77.

Guillomot M, Fléchon J-E, Wintenberger-Torres S (1981) Conceptus attachment in the ewe: an ultrastructural study. *Placenta* **2**, 169–182.

Hayat MA (1986) *Basic Techniques for Transmission Electron Microscopy*, p. 411. Orlando: Academic Press.

Hughes RL (1974) Morphological studies on implantation in marsupials. *J Reprod Fertil* **39**, 173–186.

Hughes RL, Hall LS (1984) Embryonic development in the common brushtail possum, *Trichosurus vulpecula*. In: *Possums and Gliders* (eds. Smith AP, Hume ID), pp. 197–212. Sydney: Surrey Beatty and Sons and the Australian Mammal Society.

Hulstaert CE, Kalicharan D, Hardonk MJ (1983) Cytochemical demonstration of phosphatases in the rat liver by a cerium-

based method in combination with osmium tetroxide and potassium ferrocyanide postfixation. *Histochemistry* **78**, 71–79.

Laird MK, Thompson MB, Murphy CR, et al. (2014) Uterine epithelial cell changes during pregnancy in a marsupial (*Sminthopsis crassicaudata*; Dasyuridae). *J Morphol* **275**, 1081–1092.

McAllan BM (2003) Timing of reproduction in carnivorous marsupials. In: *Predators With Pouches: The Biology of Carnivorous Marsupials* (eds Jones M, Dickman C, Archer M), pp. 147–164. Clayton, Victoria: CSIRO publishers.

McAllan BM (2011) Reproductive endocrinology of prototherians and metatherians. In: *Hormones and Reproduction of Vertebrates* (eds. Norris DO, Lopez KH), Vol. 5. (Mammals), pp. 195–214. New York: Elsevier.

Mess A (2014) Placental evolution within the supraordinal clades of Eutheria with the perspective of alternative animal models for human placentation. *Adv Biol*. doi: 10.3945/jn.112. 172148

Moffett A, Loke C (2006) Immunology of placentation in eutherian mammals. *Nat Rev Immunol* **6**, 584–594.

Mossman HW (1987) *Vertebrate Fetal Membranes: Comparative Ontogeny and Morphology; Evolution; Phylogenetic Significance; Basic Functions; Research Opportunities*. London: Macmillan.

Murphy CR (1998) Commonality within diversity: the plasma membrane transformation of uterine epithelial cells during early placentation. *J Assist Reprod Genet* **15**, 179–183.

Murphy CR, Hosie MJ, Thompson MB (2000) The plasma membrane transformation facilitates pregnancy in both reptiles and mammals. *Comp Biochem Physiol A* **127**, 433–439.

Murphy CR (2004) Uterine receptivity and the plasma membrane transformation. *Cell Res* **14**, 259–267.

Paria BC, Reese J, Das SK, et al. (2002) Deciphering the cross-talk of implantation: advances and challenges. *Science* **296**, 2185–2188.

Pilton PE, Sharman GB (1962) Reproduction in the marsupial *Trichosurus vulpecula*. *J Endocrinol* **25**, 119–136.

Potts DM, Racey PA (1971) A light and electron microscopic study of early development in the bat *Pipistrellus pipistrellus*. *Micron* **2**, 322–348.

Renfree MB (1980) Placental functions and embryonic development in marsupials. In: *Comparative Physiology: Primitive Mammals* (eds Schmidt-Nielsen K, Bollis L, Taylor CR), pp. 269–284. Cambridge: Cambridge University Press.

Renfree MB (2000) Maternal recognition of pregnancy in marsupials. *Rev Reprod* **5**, 6–11.

Renfree MB, Shaw G (2000) Diapause. *Annu Rev Physiol* **62**, 353–375.

Roberts CT, Breed WG (1994) Placentation in the dasyurid marsupial, *Sminthopsis crassicaudata*, the fat-tailed dunnart, and notes on placentation of the didelphid, *Monodelphis domestica*. *J Reprod Fertil* **100**, 105–113.

Rothchild I (2003) The yolkless egg and the evolution of eutherian viviparity. *Biol Reprod* **68**, 337–357.

Schlafke S, Enders AC (1975) Cellular basis of interaction between trophoblast and uterus at implantation. *Biol Reprod* **12**, 41–65.

Selwood L, Woolley PA (1991) A timetable of embryonic development, and ovarian and uterine changes during pregnancy in the stripe-faced dunnart, *Sminthopsis macroura* (Marsupialia: Dasyuridae). *J Reprod Fertil* **91**, 213–227.

Shaw G, Renfree MB (2006) Parturition and perfect prematurity: birth in marsupials. *Aust J Zool* **54**, 139–149.

Shorey CD, Hughes RL (1973) Development, function, and regression of the corpus luteum in the marsupial *Trichosurus vulpecula*. *Aust J Zool* **21**, 477–489.

Sizemore RJ, Hurst PR, McLeod BJ (2004) Effect of steroid hormones on tissue remodelling and progesterone receptors in the uterus of seasonally anoestrous brushtail possums (*Trichosurus vulpecula*). *Reproduction* **127**, 255–264.

Tyndale-Biscoe CH (1955) Observations on the reproduction and ecology of the brush-tailed possum, *Trichosurus vulpecula* Kerr (Marsupialia), New Zealand. *Aust J Zool* **3**, 162–184.

Tyndale-Biscoe CH (2005) *Life of Marsupials*. Clayton, Victoria: CSIRO Publishing.

Tyndale-Biscoe CH, Renfree MB (1987) *Reproductive Physiology of Marsupials*. Cambridge: Cambridge University Press.

Wildman DE (2016) IFPA Award in placentology lecture: phylogenomic origins and evolution of the mammalian placenta. *Placenta* **48(Suppl 1)**, S31–39.

Winterhager E, Denker H-W (1990) Changes in lipid organization of uterine epithelial cell membranes at implantation in the rabbit. *Troph Res* **4**, 323–338.

Wooding FBP, Burton GJ (2008) *Comparative Placentation*. Berlin: Springer-Verlag.

Wooding FBP, Flint APF (1994) Placentation. In: *Marshall's Physiology of Reproduction, Part 1* (ed. Lamming GE), pp. 233–460. London: Chapman and Hall.

Wooding FBP, Morgan G (1995) Cellular interactions during implantation in ruminants. In: *Molecular and Cellular Aspects of Peri-Implantation Processes* (ed. Dey SK), pp. 153–167. New York: Springer Verlag.

Wu Q, Thompson MB, Murphy CR (2011) Changing distribution of cadherins during gestation in the uterine epithelium of lizards. *J Exp Zool* **316**, 440–450.

Zeller U, Freyer C (2001) Early ontogeny and placentation of the grey short-tailed opossum, *Monodelphis domestica* (Didelphidae: Marsupialia): contribution to the reconstruction of the marsupial morphotype. *J Zoolog Syst Evol Res* **39**, 137–158.

Zhang S, Kong S, Lu J, et al. (2013) Deciphering the molecular basis of uterine receptivity. *Mol Reprod Dev* **80**, 8–21.